

Fluorinated Waterborne Shape Memory Polyurethane Urea for Potential Medical Implant Application

Zi Wang, Zhongyu Hou, Yanfang Wang

National Key Laboratory of Micro/Nano Fabrication Technology, Institute of Micro/Nano Science and Technology, Shanghai Jiao Tong University, Shanghai 200240, China

Correspondence to: Z. Wang (E-mail: ziwang@sjtu.edu.cn)

ABSTRACT: A series of crosslinked fluorinated waterborne shape memory polyurethane urea (PUU) ionomers were synthesized from polycaprolactone diol, perfluoropolyether (PFPE) diol, dimethylolproionic acid, isophorone diisocyanate, ethylenediamine (EDA), and diethylenetriamine (DETA). The effect of PFPE content in the soft segment and the degree of crosslinking on the molecular structure and the properties of these PUU films was examined and studied. Differential scanning calorimetry showed that the transition temperature for these T_m type shape memory PUU could be fine tuned by PFPE weight percentage and EDA/DETA ratio in the range between 33 and 44°C, covering the range of body temperature. Although incorporating amorphous fluorinated units into semicrystalline soft segment compromised the shape memory performance of PUU with linear structure as expected, the introduction of crosslinking structure using DETA as a trifunctional chain extender could still retain quite high strain recovery rate (above 90%) at 100% stretching deformation. Furthermore, the relationship of these properties as well as thermal stability with hydrogen bonding was also discussed by evaluation of the carbonyl stretching region in Fourier transform infrared spectra. © 2012 Wiley Periodicals, Inc. *J. Appl. Polym. Sci.* 000: 000–000, 2012

KEYWORDS: shape memory polymer; fluorinated polymer; waterborne polyurethane urea; crosslinking; hydrogen bonding

Received 3 February 2012; accepted 9 April 2012; published online

DOI: 10.1002/app.37862

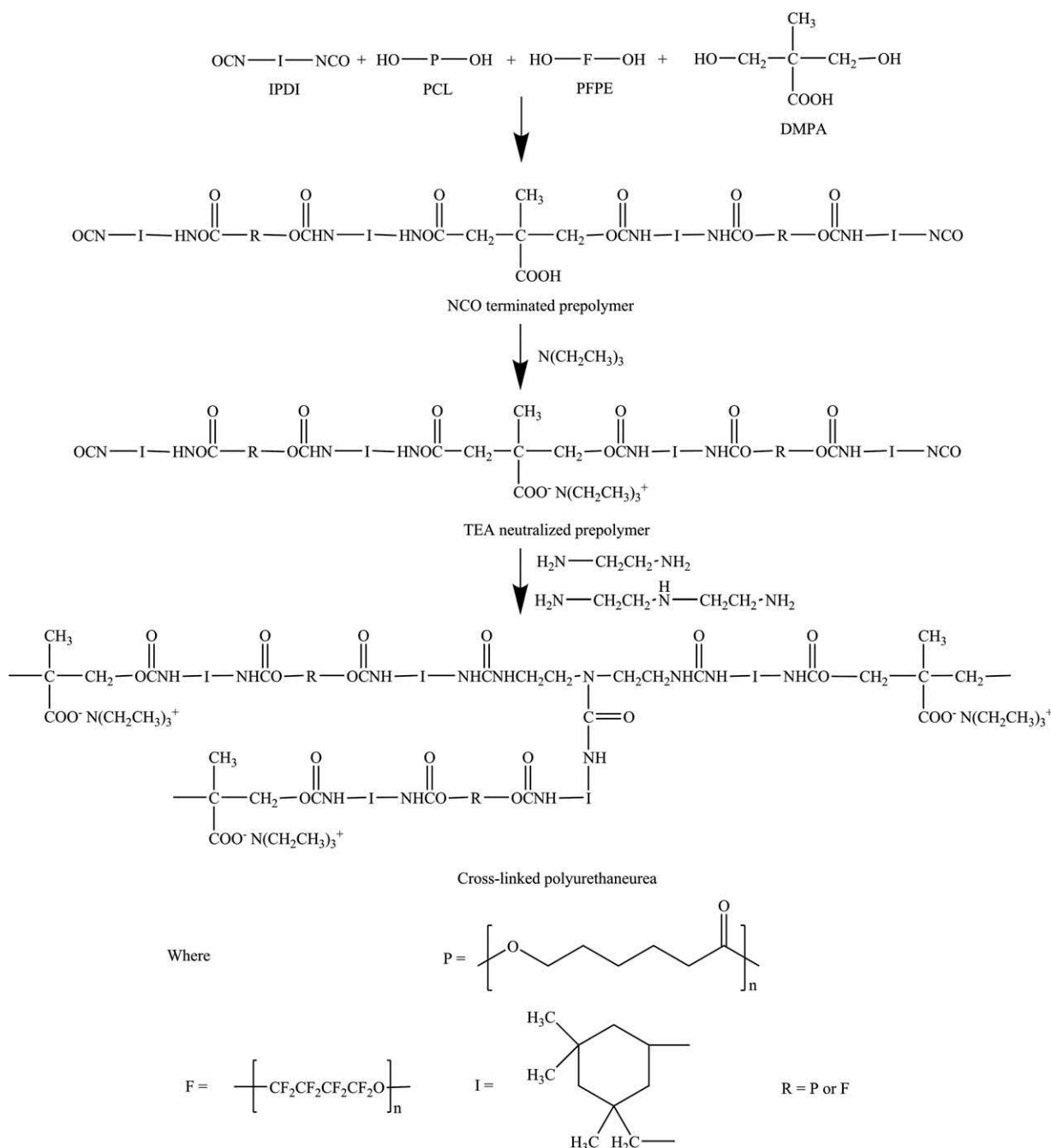
INTRODUCTION

Percutaneous transluminal coronary angioplasty is one of the most effective therapies for curing coronary diseases. Although restenosis rate within 6 months is high as 30–40%, stents providing intra-arterial support can effectively decrease the restenosis rate to 20–30%.^{1,2} Thermally induced shape memory materials can recover from their temporary shape to permanent shape in certain temperature range,^{3,4} showing great potential for their application as medical implant materials including coronary stents.⁵ Nitinol (Ni-Ti) and other shape memory alloys have demonstrated outstanding properties, such as small size and high strength, and they have been used for fabricating self-expanding stents competing with traditional stainless steel stents.^{5,6} However, their relatively high cost, limited recoverable deformation, and possible toxicity through releasing metal ions restrict their extensive application to some extent.^{5–7} In comparison with alloys, shape memory polymers (SMPs) have much larger recoverable deformation. Their properties can be easily tailored by flexible combination of various monomers and polymerization routines.

Thermally induced SMP is composed of switchable molecular segments crosslinked by chemical or physical netpoints. The switchable molecular segments allow the material to be deformed and then fixed to a temporary shape, and the netpoints can make the material recover to its permanent shape when the temperature is above the transition point of the switchable molecular segments (glass transition temperature T_g or melting temperature T_m). Segmented polyurethane (PU) and polyurethane urea (PUU), with oligomeric diol as soft segments linked by hard segments composed of highly polar urethane and urea groups, are therefore appropriate candidates for shape memory materials. They belong to a versatile class of polymers whose properties can be tuned by flexible choices of oligomeric diol, diisocyanates, and chain extenders. Recently, various shape memory PU showing suitable for biomedical application have been synthesized, which are based on poly(ϵ -caprolactone) (PCL),^{8–11} oligo[(*rac*-lactide)-*co*-glycolide],^{12,13} and poly(*rac*-lactide).¹⁴

One of the prerequisites for SMP to be used as ideal stent materials is that its thermal switching temperature needs to be close

© 2012 Wiley Periodicals, Inc.



Scheme 1. The synthesis of fluorinated waterborne shape memory PUU.

to the body temperature. Recently, Lendlein et al.¹⁴ synthesized a series of shape memory PU based on poly(*rac*-lactide) copolymers. By incorporation of different comonomer and tuning their ratios in the synthesis of poly(*rac*-lactide)-based macropolyols, the thermal switching temperature (T_g type) could be adjusted between 14 and 56°C. The same group also reported a polymer network based on oligo[ϵ -caprolactone]-co-glycolate dimethylacrylates and butyl acrylate with glycolate content between 0 and 30 mol %, in which the T_m could be adjusted between 18 and 53°C.¹⁵ Ahmad et al.¹⁶ reported that T_g as transition temperature could also be tuned by controlling the hard

segment content of PU. In terms of coronary stents application, lowering the surface energy is also important for preventing the unfavorable blood deposits from precipitating on stent surface. Conversely, fluorinated PU and PUU coatings have long been recognized for waterproofing or other scenarios where low surface energy is required.^{17,18} From this point of view, shape memory PU or PUU incorporated with fluorinated segments with thermal response around body temperature should be one of the ideal materials for coronary stents. However, to our best knowledge, the reports on fluorinated SMP especially shape memory PU (or PUU) are few.

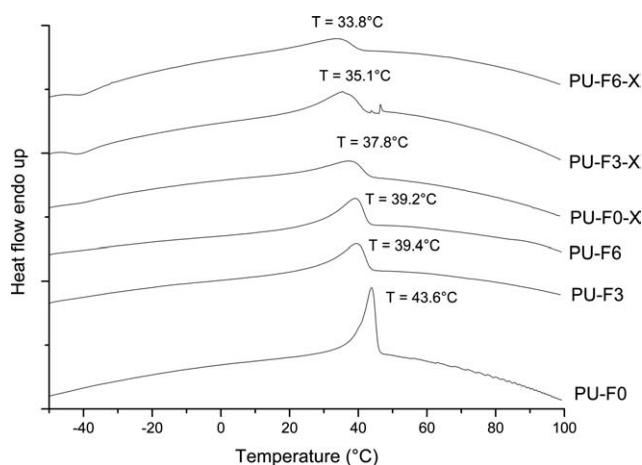


Figure 1. DSC curves of PUU samples with linear structure and cross-linked structure.

In this article, we report the synthesis of perfluoropolyether (PFPE)-modified shape memory waterborne PUU based on commercially available PCL diol (industrial grade). By tuning the content of PFPE in soft segments and the trifunctional chain extender, the T_m could be adjusted between 33 and 44°C. Although incorporating fluorinated units into semicrystalline soft segment compromised the shape memory performance of PUU with linear structure as expected, the introduction of crosslinking structure using diethylenetriamine (DETA) could still retain quite high strain recovery rate (above 90%) at 100% stretching deformation.

EXPERIMENTAL

PFPE ($M_n = 3800$), dimethylolproionic acid (DMPA), isophorone diisocyanate (IPDI), and dibutyltin dilaurate (DBTDL) were standard reagents purchased from Sigma-Aldrich, Shanghai, China. PCL ($M_n = 4000$) was an industrial product from Solvey. Triethylamine (TEA), ethylenediamine (EDA), DETA, and dimethylformamide (DMF) were analytical grade reagents, offered by Shanghai chemical reagent company, Shanghai, China, and treated with 4 Å molecular sieves for 1 week before use. PCL and DMPA were dried *in vacuo* at 90°C for 2 h to remove any residual moisture. Other materials were used as received.

A stoichiometric amount of PCL, PFPE, DMPA, and IPDI ($[\text{NCO}]/[\text{OH}]$ molar ratio = 1.8) dissolved in 20 mL of DMF were charged into a 250-mL four-necked flask equipped with a nitrogen inlet, a condenser, a thermometer, and a mechanical stirrer. After one drop of DBTDL was added as catalyst, the reaction was performed at 85°C until the theoretical NCO value was reached (about 4–5 h). Then, the NCO-terminated prepolymer was neutralized by TEA at 40°C for 20 min and dispersed into deionized water under vigorous agitation. Finally, a stoichiometric amount of EDA and DETA dissolved in deionized water was added for chain extension. The whole synthetic process was shown in Scheme 1. The DMPA and hard segment contents were 4 and 30 wt % based on total mass of polymer, respectively. The solid content for all the aqueous dispersion samples was 20%. The PUU films were prepared by casting the disper-

sion into a Teflon mold at ambient temperature. Then, they were dried at 30°C for 4 days and *in vacuo* at 60°C for 24 h.

The differential scanning calorimetry (DSC) curves were recorded on a Perkin Elmer Diamond DSC Analyzer at a heating rate of 10°C/min purged with nitrogen gas. The thermal stability of samples were tested on a Perkin Elmer Pyris 1 thermogravimetric analyzer (TGA) at a heating rate of 10°C/min under nitrogen atmosphere. The Fourier transform infrared (FTIR) absorption spectra were obtained on a Bruker Vertex 70 system. The samples were cast from 3 wt % DMF solution on a KBr plate, followed by vacuum drying under 80°C to rapidly remove the solvent. The spectra were analyzed using Bruker OPUS 6.5 Software. Curve fitting on the carbonyl stretching region was performed according to the procedure described previously.¹⁹ The strain recovery rate were measured on a TA Q800 dynamic mechanical analyzer.

RESULTS AND DISCUSSION

Crystallization and Melting Temperature Tuning

It is well known that the capability of thermally induced SMP is to fix a temporary shape and to recover an original shape using of heat stimuli. Shape fixing stores strain energy by cooling below a certain switching temperature, by which the material can retain a temporary shape. This process results from a transition between a state in which changes in conformational entropy are dominant (entropic rubber) and the other state with limited chain mobility.²⁰ At the molecular level, shape fixing can be achieved by designed crystallization or vitrification of the constituent chains at a targeted thermal switching temperature. Other methods to immobilize the chains, for example, by the establishment of a secondary and labile crosslinked network, are also applicable. The permanent shape of SMP can be recovered from its temporarily fixed shape by heating above the thermal switching temperature. In the case of segmented PU or PUU, this capability results from the microphase separation owing to the existence of hard segments and soft segments in PUU molecular chains. For the PUU studied here, the hard segments are composed of DMPA–IPDI–EDA or DMPA–IPDI–DETA units, and these highly polar urethane and urea linkages can restore the material to its permanent shape above the thermal switching temperature. Semicrystalline PCL or PCL–PFPE chains are soft segments, which fix the material to its temporary shape below the thermal switching temperature. Obviously, this type of PUU should demonstrate shape recovering behavior around the T_m of semicrystalline soft segments. Therefore, fine tuning of thermal switching temperature can be achieved by disrupting the main chain packing and raising their crystallization potential barrier, aiming at partially suppressing the crystallization of soft segments.

As shown in Figure 1, the crystallization of soft segment were investigated by DSC, and the experimental results for melting temperature tuning were summarized in Table I. Linear structured PU-F0 with PCL diol ($M_w = 4000$) alone as soft segment was first studied as a control sample. The T_m of soft segment was 43.6°C, which appeared as a sharp peak on DSC curve. The measured crystallinity ($X_c = 25.4\%$) and melting enthalpy (35.6 J mol⁻¹) were also consistent with those reported in previous

Table I. Results of Crystallization and Melting Temperature Tuning for Fluorinated PUU with Linear Structure and Cross-Linked Structure

Sample	PFPE ^a (wt %)	DETA ^b (mol %)	T_m^c (°C)	ΔH^d (J/mol)	X_c^e (%)	$R_r(5)^f$ (%)
PU-F0	0	0	43.6	35.6	25.4	91
PU-F3	3	0	39.4	31.0	22.1	82
PU-F6	6	0	39.2	24.8	17.7	80
PU-F0-X	0	50	37.8	24.6	17.6	92
PU-F3-X	3	50	35.1	28.0	20.0	93
PU-F6-X	6	50	33.8	22.2	15.8	90

^aWeight percentage versus total polymer weight, ^bMolar fraction of chain extender, ^cMelting temperature of soft segments by DSC, ^dMelting enthalpy by DSC, ^eCrystallinity of soft segments, ^fStrain recovery rate tested at fifth cycle.

article.⁹ As a small amount of PFPE diol (3 wt %) was introduced into the soft segments, X_c and T_m were reduced to 22.1% and 39.4°C, respectively. Increasing the PFPE content to 6 wt % showed limited effect on T_m (39.2°C), although X_c of soft segment was decreased further to 17.7%. These results showed that the incorporation of amorphous PFPE into soft segments could tune the thermal switching temperature quite close to the body temperature by hindering the crystallization process of PCL. Nevertheless, suppressed crystallization of soft segment showed negative effect on shape memory performance. The strain recovery rate at 100% stretching deformation was found decreased from 91 to 80% as the PFPE content increased from 0 to 6 wt %. To continue tuning down the switching temperature while maintaining the shape memory performance as possible, 50 mol % of previously used bifunctional chain extender EDA was replaced by trifunctional chain extender DETA. Compared with the control sample PU-F0, the T_m of soft segment was significantly lowered from 43.6 to 37.8°C on the adoption of cross-linked structure. Although the crystallinity of soft segment was low as 17.6%, relatively high shape memory performance was retained (92% strain recovery rate at 100% stretching deformation). Adding 3 wt % of PFPE could tune the T_m to slightly below the body temperature (35.1°C), but the crystallinity of soft segment rose slightly to 20% which might be attributed to the increased density of ordered hydrogen bonding caused by fluorinated groups (shown later in FTIR analysis). The strain recovery rate of this sample PU-F3-X reached 93%, rendering this material potential for medical implant application such as blood deposit preventing coronary stents. T_m of the soft segment could be further decreased to 33.8°C by adding 6 wt % of PFPE.

Hydrogen Bonding

In terms of the molecular structure of a segmented PUU, the strong hydrogen bonding of the urethane and urea linkages can be easily formed. Hydrogen-bonding interaction plays important role in shape recovering process, crystallization process, thermal stability, and other important properties. The formation of ordered structure of hard segments in PUU is also highly related to the hydrogen bonding and can be characterized by infrared spectroscopy.¹⁹ The region at 1750–1600 cm^{-1} corresponding to the carbonyl stretching vibration has been widely used to investigate the hydrogen bonding of the urethane and urea linkages of PUU.^{19,21–26} Considering the structure of PCL chains in soft segment, the absorption peaks for urethane groups would be

affected by the carbonyl absorption peaks of the ester groups. Therefore, only the hydrogen bonding between the urea linkages was chosen for investigation. Fortunately, the carbonyl absorption peak of DMPA embedded in hard segments was located at 1550 cm^{-1} , which had no overlap with the urea carbonyl region under investigation.^{19,21} Figure 2 shows the FTIR spectra for all the PUU samples under ambient temperature, and multiple bands could be found in carbonyl region assigned to different kinds of hydrogen bonding (see Table II). The iteration procedure of damping least squares, based on a combination of

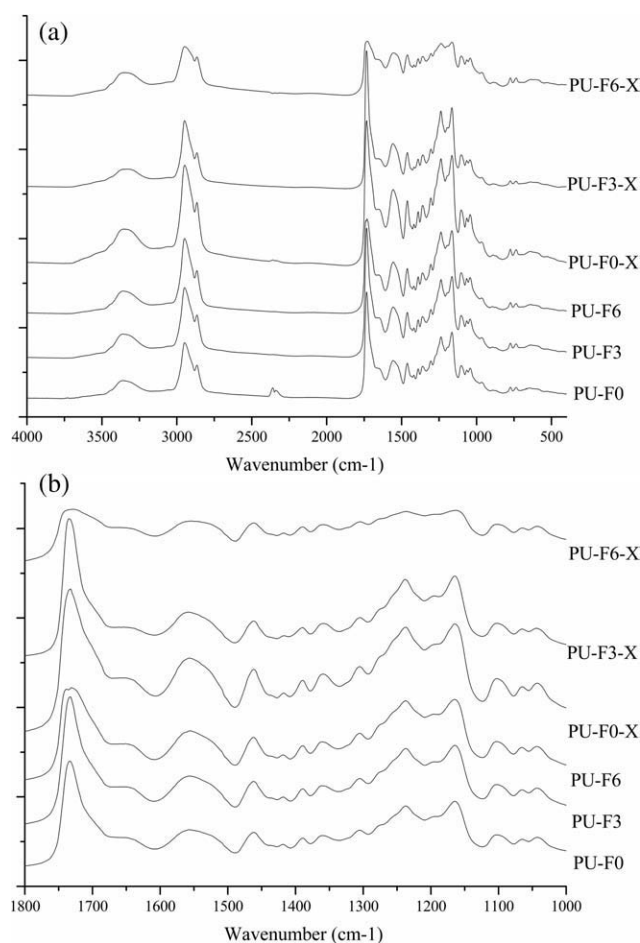


Figure 2. (a) FTIR spectra of PUU samples; (b) FTIR spectra between band 1800 and 1000 cm^{-1} .

Table II. Assignments of Absorption Bands in Carbonyl Stretching Region of FTIR for PUU

Wave number (cm ⁻¹)	Assignments
1750–1728	Free carbonyl stretching of urethane
1727–1717	Disordered hydrogen-bonded carbonyl for urethane linkages
1710–1700	Ordered hydrogen-bonded carbonyl for urethane linkages
1690–1680	Free carbonyl stretching of urea
1680–1650	Disordered hydrogen-bonded carbonyl for urea linkages
1640–1632	Ordered hydrogen-bonded carbonyl for urea linkages

Lorentzian and Gaussian curve shapes, was used to separate the absorption peaks in the carbonyl region,¹⁹ and the curve-fitting results were listed in Table III. The degree of hydrogen bonding for urea linkages ($X_{b, UA}$) and the fractions of ordered and disordered hydrogen bonds between urea groups ($X_{o, UA}$ and $X_{d, UA}$) in Table III were defined as follows:

$$X_{b, UA} = \frac{\sum \text{Area}(\text{bonded})}{\text{Area}(1690 - 1680\text{cm}^{-1}) + \sum \text{Area}(\text{bonded})} \quad (1)$$

$$X_{o, UA} = \frac{\sum \text{Area}(1640 - 1632\text{cm}^{-1})}{\text{Area}(1690 - 1680\text{cm}^{-1}) + \sum \text{Area}(\text{bonded})} \quad (2)$$

$$X_{d, UA} = \frac{\sum \text{Area}(1680 - 1650\text{cm}^{-1})}{\text{Area}(1690 - 1680\text{cm}^{-1}) + \sum \text{Area}(\text{bonded})} \quad (3)$$

In the case of PUU with linear structure, as the PFPE contents in soft segments rose from 0 to 6 wt %, $X_{b, UA}$ increased from 56.2 to 66.0%, indicating the enhancement of hydrogen-bonding interaction brought by CF₂ groups. For bonded urea groups, $X_{d, UA}$ increased from 38.4 to 47.2%, whereas $X_{o, UA}$ does not seemed to be sensitive to the fraction of fluorinated units. Owing to the strong electronegativity of fluorine atoms, the formation of hydrogen bonding between the fluorine on the –CF₂ groups of PFPE and the proton on N–H of the urea groups should be expected. Recently, Su et al.^{19,21} prepared waterborne polyester PUU with the soft segment incorporated with fluorinated polysiloxane. Their results also revealed significant increase in the degree of hydrogen bonding and the fraction of

Table III. Curve-Fitting Results of FTIR in Carbonyl Stretching Region

Samples	$X_{b, UA}$ ^a (%)	$X_{o, UA}$ ^b (%)	$X_{d, UA}$ ^c (%)
PU-F0	56.2	38.4	17.8
PU-F3	61.2	40.9	20.3
PU-F6	66.0	47.2	18.8
PU-F0-X	65.5	65.5	0.0
PU-F3-X	60.6	47.0	13.6
PU-F6-X	65.1	49.7	15.4

^aThe total degree of hydrogen bonding for urea linkages, ^bThe fraction of disordered hydrogen bonds, ^cThe fraction of ordered hydrogen bonds.

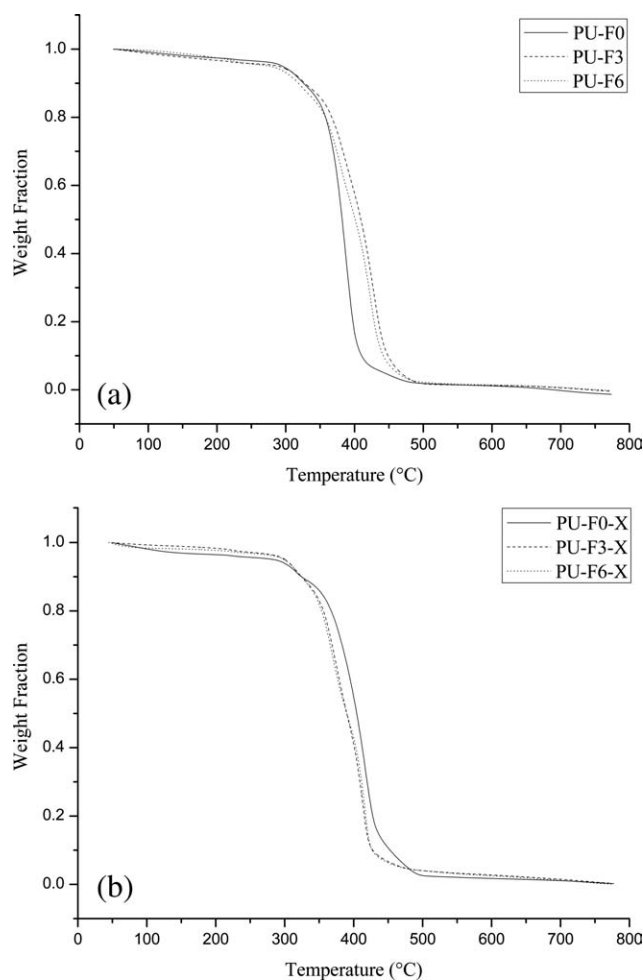


Figure 3. TGA thermographs of PUU samples: (a) with linear structures and (b) with crosslinked structures.

disordered hydrogen bonds on the introduction of fluorinated polysiloxane. Wang²⁷ performed a quantum chemical computation on the hydrogen-bonding interaction between –CF₂ groups and urethane linkages using B3LYP/6-31G basis sets. The calculated hydrogen-bonding energy between fluorine atom and urethane proton was 43.0 kJ mol⁻¹, which was 11.6 kJ mol⁻¹ lower than the self-urethane interaction. This theoretical investigation may explain the enhanced disordered hydrogen bonds on the incorporation of fluorinated segments found by Su et al.¹⁹ and our study. This relatively low hydrogen-bonding energy may also be contributed to phase mixing owing to the promoted association between hard segment urea and soft segment PFPE, thus compromising the shape memory performance as shown in DSC results. For PUU samples with crosslinked structures, even the sample PU-F0-X without fluorinated units $X_{b, UA}$ was quite high as 65.5%. However, $X_{o, UA}$ of PU-F0-X was found 0.0% that means almost all the urea hydrogen bonds formed were disordered. This phenomenon may be related to the immobilization of molecular chains by crosslinking points and should be investigated in future research. On adding 3 wt % PFPE into the soft segments, the ordered hydrogen bonds in urea linkages started to form and $X_{o, UA}$ increased to 15.6%.

Table IV. Thermal Decomposition Temperature at Different Weight Losses by TGA^a

Sample	$T_{d,5\%}$ (°C)	$T_{d,10\%}$ (°C)	$T_{d,25\%}$ (°C)	$T_{d,40\%}$ (°C)	$T_{d,50\%}$ (°C)	$T_{d,60\%}$ (°C)	$T_{d,75\%}$ (°C)
PU-F0	295	326	364	376	382	387	395
PU-F3	289	329	376	397	409	419	431
PU-F6	277	318	367	387	401	412	425
PU-F0-X	284	324	376	395	404	412	423
PU-F3-X	300	324	363	379	390	401	412
PU-F6-X	299	324	360	377	389	403	415

^a $T_{d, x\%}$ means thermal decomposition temperature at X% weight loss.

Further investigation on the effect of highly polar fluorinated groups on the hydrogen-bonding interactions of PUUs and their shape memory performance is necessary.

Thermal Stability

The TGA thermographs of PUU samples with linear structure and crosslinked structure were listed in Figure 3(a, b), respectively, and the data for thermal decomposition temperature (T_d) at different weight losses (e.g., $T_{d,5\%}$ means T_d at 5% weight loss) were also summarized in Table IV. Figure 3(a) showed that in the range of 20–80% weight loss the T_d of PU-F3 and PU-F6 was about 10–30°C higher than PU-F0 at the same weight loss. In the range below 10% weight loss, the T_d of PU-F3 was almost the same as that of PU-F0. This phenomenon was very similar with that reported by Zhu et al.,²⁸ in which a telechelic PU end-capped with PFPE was synthesized. This improved thermal stability of fluorinated PUU was in consistence with the enhancement of hydrogen-bonding interaction brought by PFPE shown by FTIR spectra, which has been already discussed above. Although the incorporation of PFPE into soft segments could offer higher thermal stability for PUU with linear structure, the situation was found almost reversed for PUU with crosslinked structure. Figure 3(b) showed that the T_d of PU-F3-X and PU-F6-X was about 10–15°C lower than PU-F0-X in the range of 20–80% weight loss, although in the range below 10% weight loss, the T_d of the two fluorinated samples was found to be 10–15°C higher. Further investigation on these results and their dependence on hydrogen-bonding interaction is necessary.

CONCLUSIONS

In conclusion, a series of fluorinated waterborne shape memory PUU ionomers with linear structure or crosslinked structure were synthesized. The experimental results showed that the thermal switching temperature of PUU could be fine tuned by PFPE weight percentage and EDA/DETA ratio in the range between 33 and 44°C, covering the range of body temperature. Through the introduction of crosslinked structure, the strain recovery rate could be retained above 90%, effectively compensating the negative effect on shape memory performance brought by PFPE segments. The analysis of urea carbonyl region on FTIR spectra found significant enhancement of hydrogen-bonding interaction on the addition of PFPE for PUU with linear structure. Furthermore, adding a small

amount of PFPE could improve the thermal stability of PUU with linear structure.

ACKNOWLEDGMENTS

Financial support from Natural Science Foundation of China under Grant No. 60807008 and Natural Science Foundation of Shanghai under Grant No. 08520741500 was appreciated.

REFERENCES

- Serruys, P. W.; Jaegers, P. D.; Kiemeneij, F.; Macaya, C.; Rutsch, W.; Heyndrickx, G.; Emanuelsson, H.; Marco, J.; Legrand, V.; Materne, P.; Belardi, J.; Sigwart, U.; Colombo, A.; Goy, J. J.; van den Heuvel, P. Delcan, J.; Morel, M. N. *Engl. J. Med.* **1994**, *331*, 489.
- Fischman, D. L.; Leon, M. B.; Baim, D. S.; Schatz, R. A.; Savage, M. P.; Penn, I.; Detre, K.; Veltri, L.; Ricci, D.; Nobuyoshi, M.; Cleman, M.; Heuser, R.; Almond, D.; Teirstein, P. S.; Fish, R. D.; Colombo, A.; Brinker, J.; Moses, J.; Shakhovich, A.; Hirshfeld, J.; Bailey, S.; Ellis, S.; Rake, R.; Goldberg, S. N. *Engl. J. Med.* **1994**, *331*, 496.
- Behl, M.; Lendlein, A. *Mater. Today* **2007**, *10*, 20.
- Behl, M.; Lendlein, A. *Soft Matter* **2007**, *3*, 58.
- Mani, G.; Feldman, M. D.; Patel, D.; Agrawal, C. M. *Biomaterials* **2007**, *28*, 1689.
- Langer, R.; Tirrell, D. A. *Nature* **2004**, *428*, 487.
- Heintz, C.; Riepe, G.; Birken, L.; Kaiser, E.; Chakfé, N.; Morlock, M.; Delling, G.; Imig, H. J. *Endovasc. Ther.* **2001**, *8*, 248.
- Lendlein, A.; Langer, R. *Science* **2002**, *296*, 1673.
- Ping, P.; Wang, W.; Chen, X.; Jing, X. *Biomacromolecules* **2005**, *6*, 587.
- Ajili, S. H.; Ebrahimi, N. G.; Soleimani, M. *Acta Biomater.* **2009**, *5*, 1519.
- Feng, Y.; Behl, M.; Kelch, S.; Lendlein, A. *Macromol. Biosci.* **2009**, *9*, 45.
- Alteheld, A.; Feng, Y.; Kelch, S.; Lendlein, A. *Angew. Chem. Int. Ed.* **2005**, *44*, 1188.
- Wischke, C.; Neffe, A. T.; Steuer, S.; Lendlein, A. J. *Control. Release* **2009**, *138*, 243.
- Lendlein, A.; Zotzmann, J.; Feng, Y.; Alteheld, A.; Kelch, S. *Biomacromolecules* **2009**, *10*, 975.

15. Kelch, S.; Steuer, S.; Schmidt, A. M.; Lendlein, A. *Biomacromolecules* **2007**, *8*, 1018.
16. Ahmad, M.; Luo, J.; Xu, B.; Purnawali, H.; King, P. J.; Chalker, P. R.; Fu, Y.; Huang, W.; Mirafatab, M. *Macromol. Chem. Phys.* **2011**, *212*, 592.
17. Trombetta, T.; Iengo, P.; Turri, S. J. *Appl. Polym. Sci.* **2005**, *98*, 1364.
18. Wu, W.; Zhu, Q.; Qing, F.; Han, C. C. *Langmuir* **2009**, *25*, 17.
19. Su, T.; Wang, G. Y.; Xu, X. D.; Hu, C. P. *J. Polym. Sci. Part A: Polym. Chem.* **2006**, *44*, 3365.
20. Mather, P. T.; Luo, X.; Rousseau, I. A. *Annu. Rev. Mater. Res.* **2009**, *39*, 445.
21. Su, T.; Wang, G. Y.; Hu, C. P. *J. Polym. Sci. Part A: Polym. Chem.* **2006**, *44*, 5005.
22. Coleman, M. M.; Lee, K. H.; Skrovanek, D. J. *Painter, P. C. Macromolecules* **1986**, *19*, 2149.
23. Hu, Y. S.; Tao, Y.; Hu, C. P. *Biomacromolecules* **2001**, *2*, 80.
24. Luo, N.; Wang, D. N.; Kang, Y. S. *Macromolecules* **1997**, *30*, 4405.
25. Wang, G. Y.; Zhu, M. Q.; Hu, C. P. *J. Polym. Sci. Part A: Polym. Chem.* **2000**, *38*, 136.
26. Yang, D. Y.; Hu, C. P.; Ying, S. K. *J. Polym. Sci. Part A: Polym. Chem.* **2005**, *43*, 2606.
27. Wang, L. *-F. Polymer* **2007**, *48*, 894.
28. Zhu, Q.; Han, C. C. *Polymer* **2010**, *51*, 877.